Supplemental Information

Metal-ion-mediated synergistic coordination: Construction of AIE metallogel sensor array for anions and amino acids

Hong Yao*[a], Yan-Bing Niu[a], Yin-Ping Hu[a], Xiao-Wen Sun[a], Qin-Peng Zhang[a], You-Ming Zhang[a,b], Tai-Bao Wei[a] and Qi Lin*[a]

[a] *Key Laboratory of Eco-Functional Polymer Materials of the Ministry of Education, Key Laboratory of Polymer Materials of Gansu Province, College of Chemistry and Chemical Engineering, Northwest Normal University, Lanzhou, Gansu, 730070. P. R. China*

[b] *Gansu Natural Energy Research Institute, Lanzhou, Gansu 730046, China*

---

* Corresponding author

* E-mail: yhxbz@126.com, linqi2004@126.com.

Table of Contents

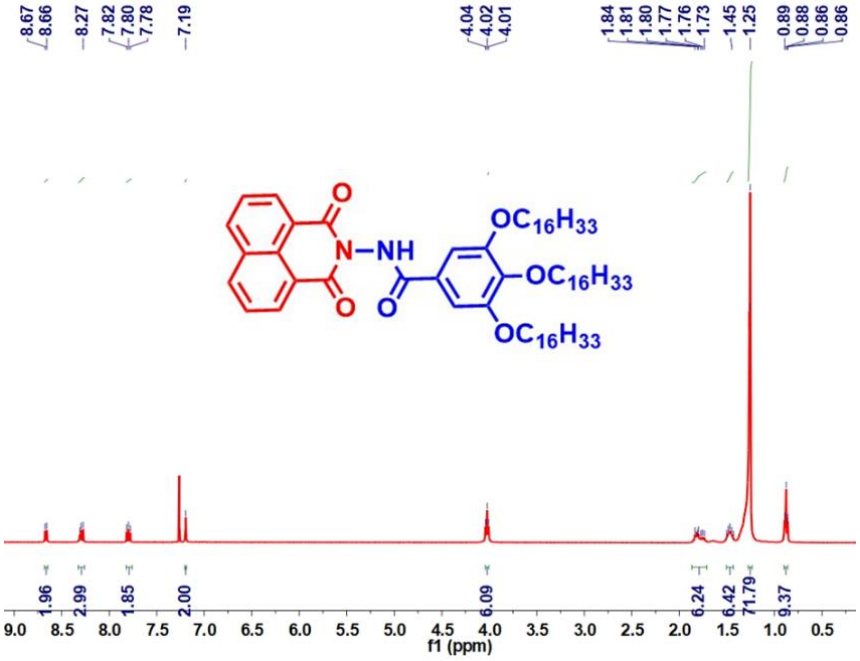

Fig. S1 The ^{1}H NMR spectra of gelator **G** in $CDCl_3$ (400 MHz, 298K).

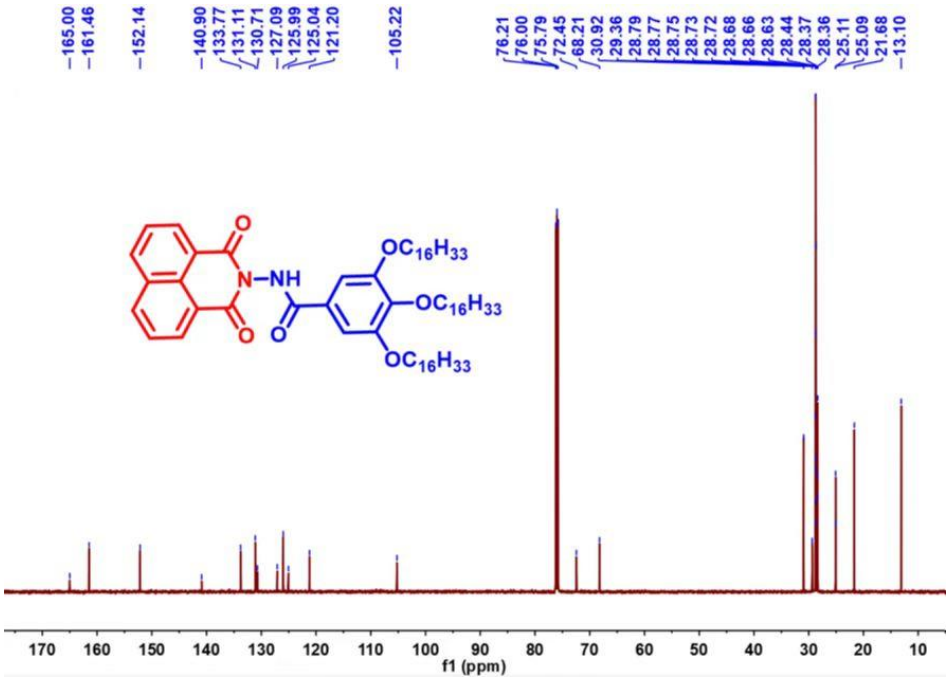

Fig. S2 The ^{13}C NMR spectra of gelator **G** in $CDCl_3$ (600 MHz, 298K).

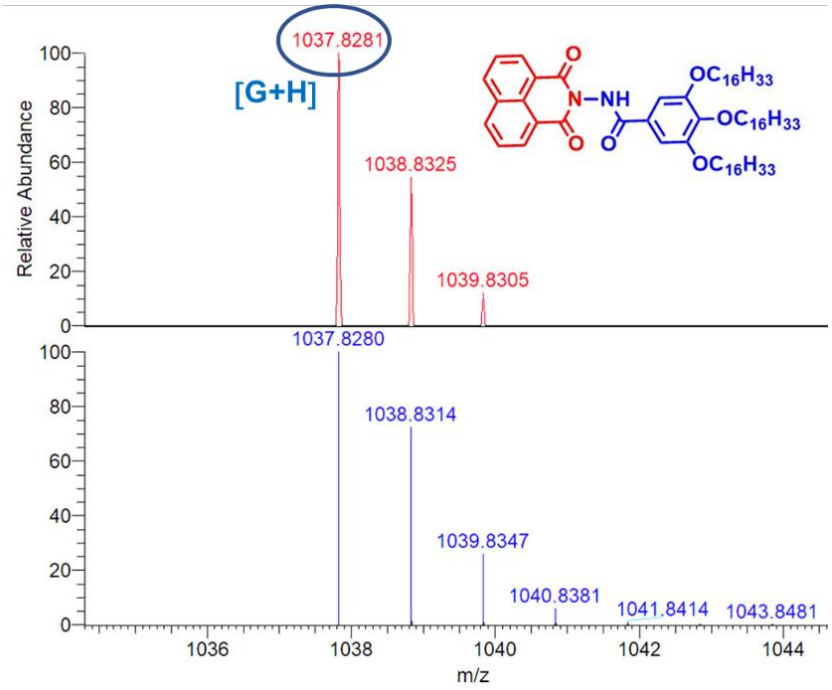

Fig. S3 ESI-MS spectra of gelator **G**.

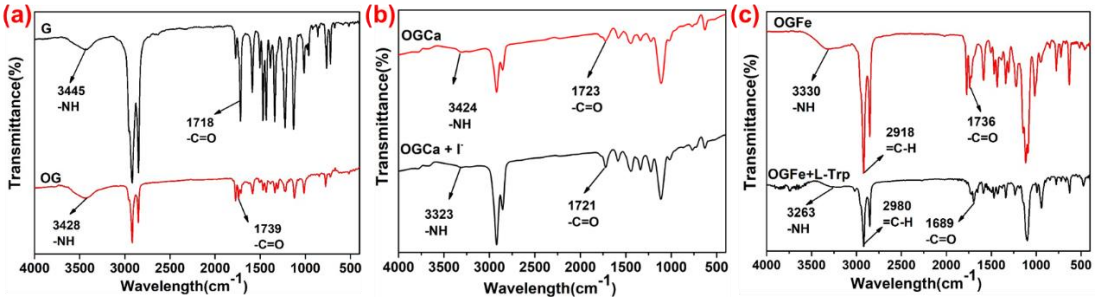

Fig. S4 FT-IR spectra of (a) Powder **G** and xerogel **OG**，(b) Metallogel **OGCa** and **OGCa-I**¯，(c) Metallogel **OGFe** and **OGFe-Trp**.

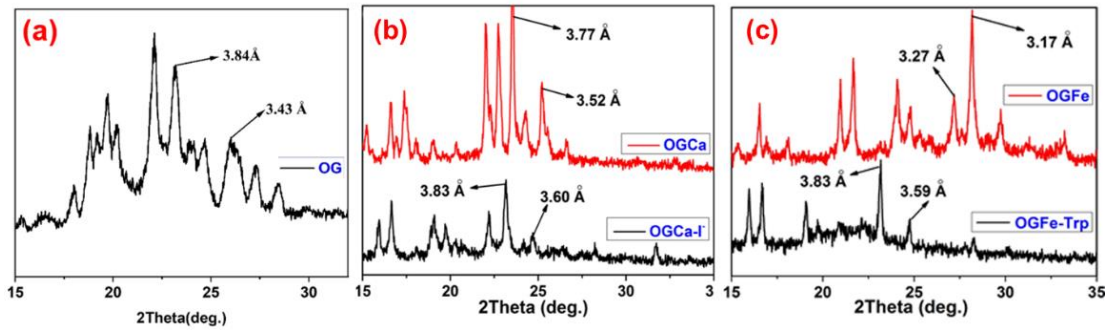

Fig. S5 XRD patterns of (a) Powder **G** and xerogel **OG**，(b) Metallogel **OGCa** and **OGCa-I**¯, (c) Metallogel **OGFe** and **OGFe-Trp**.

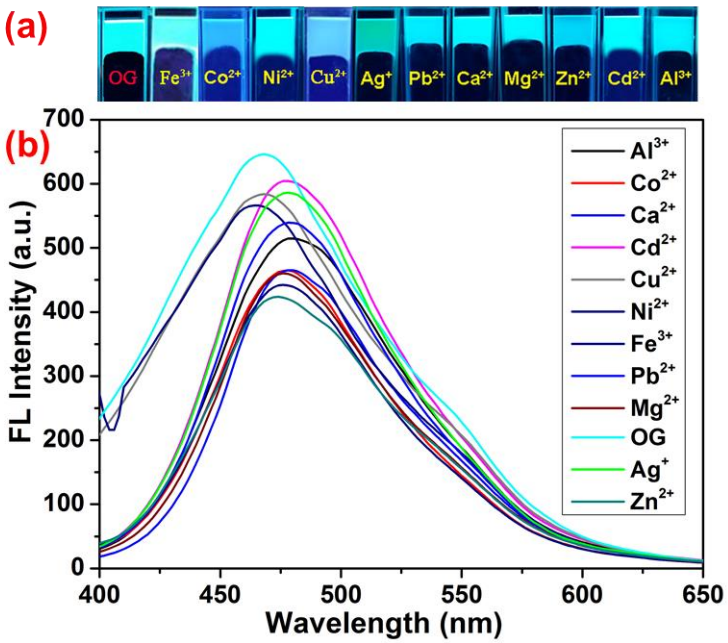

Fig. S6 (a) Images of **OG** and **OG** in the presence of 1.0 equiv. various metal ions (using their perchlorate salts as the sources) under ultraviolet light (UV) in cyclohexanol solution (5%, w/v); (b) Fluorescent spectra of **OG** and **OGMs** (λex = 365 nm).

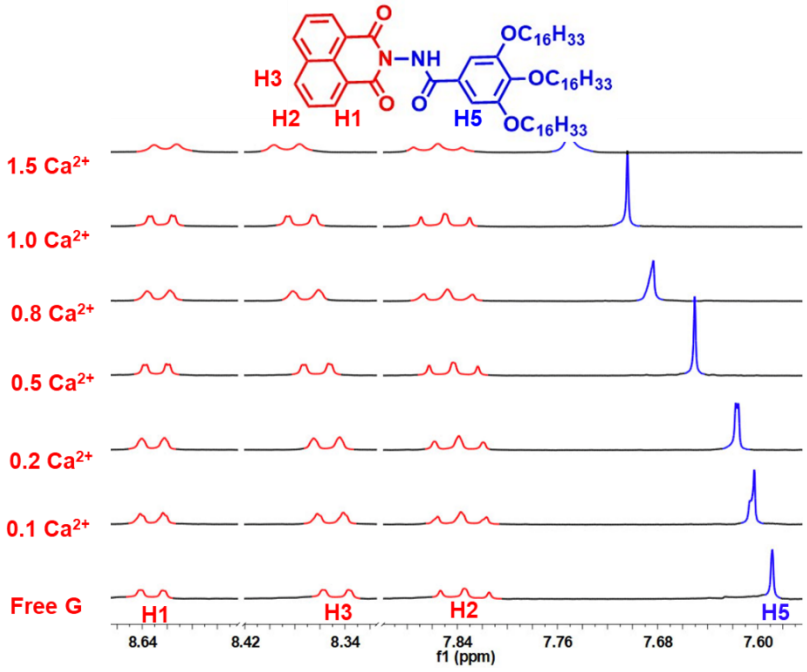

Fig. S7 ^{1}H NMR titration spectra (400 MHz, 298 K) of **OG (**5.0 mg**)** $CDCl_3$ (0.5ml) and DMSO-d_6 (0.1ml) solution with increasing amounts of **Ca**$^{2+}$(DMSO-*d6*, 0.1M).

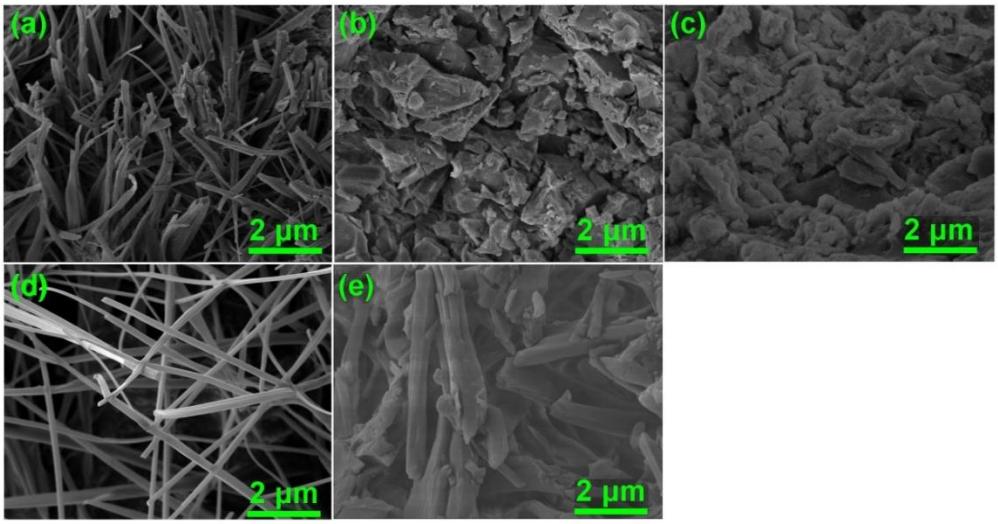

Fig. S8 SEM images of (a) Xerogel **OG**, (b) Metallogel **OGCa**, (c) Metallogel complex **OGCa-I**$^-$, (d) Metallogel **OGFe**, (e) Metallogel complex **OGFe-Trp**.

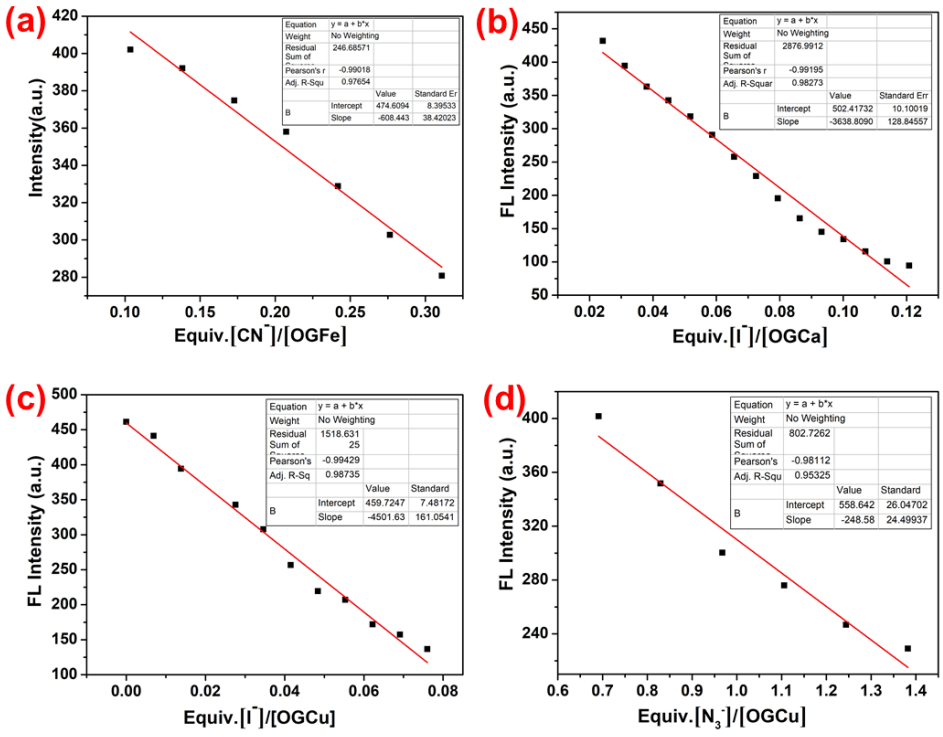

Fig. S9 The photograph of the linear range: (a) Metallogel **OGFe** with CN^-, (b) **OGCa** with I^-, (c) **OGCu** with I^-, (d) **OGCu** with N_3^-.

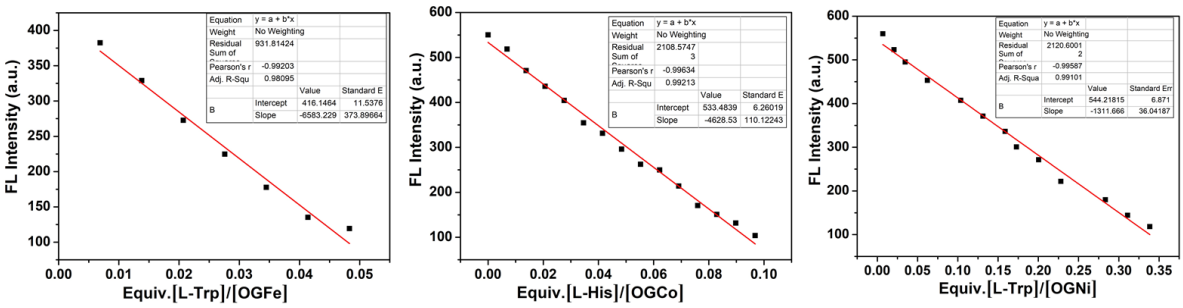

Fig. S10 The photograph of the linear range: (a) Metallogel **OGFe** with L-Trp, (b) **OGCo** withL-His, (c) **OGNi** with L-Trp.

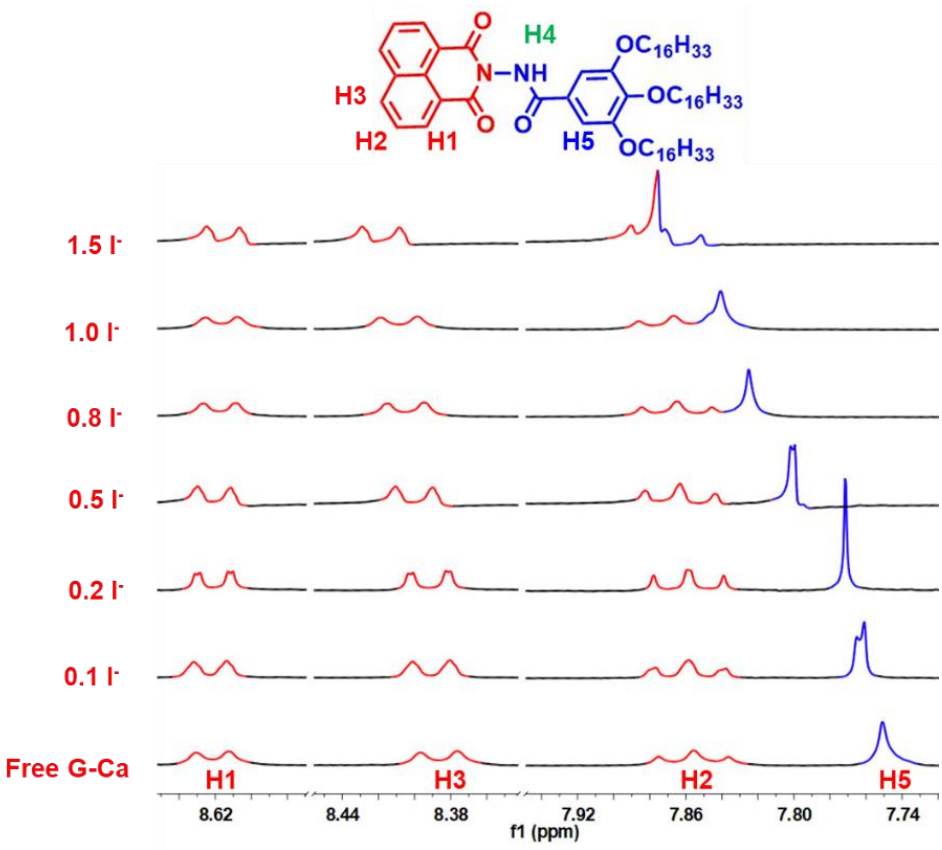

Fig. S11 ^{1}H NMR titration spectra (400 MHz, 298 K) of **OGCa (**5.0 mg**)** in $CDCl_3$ (0.5mL) and DMSO-d_6 (0.1ml) solution with increasing amounts of I^-.

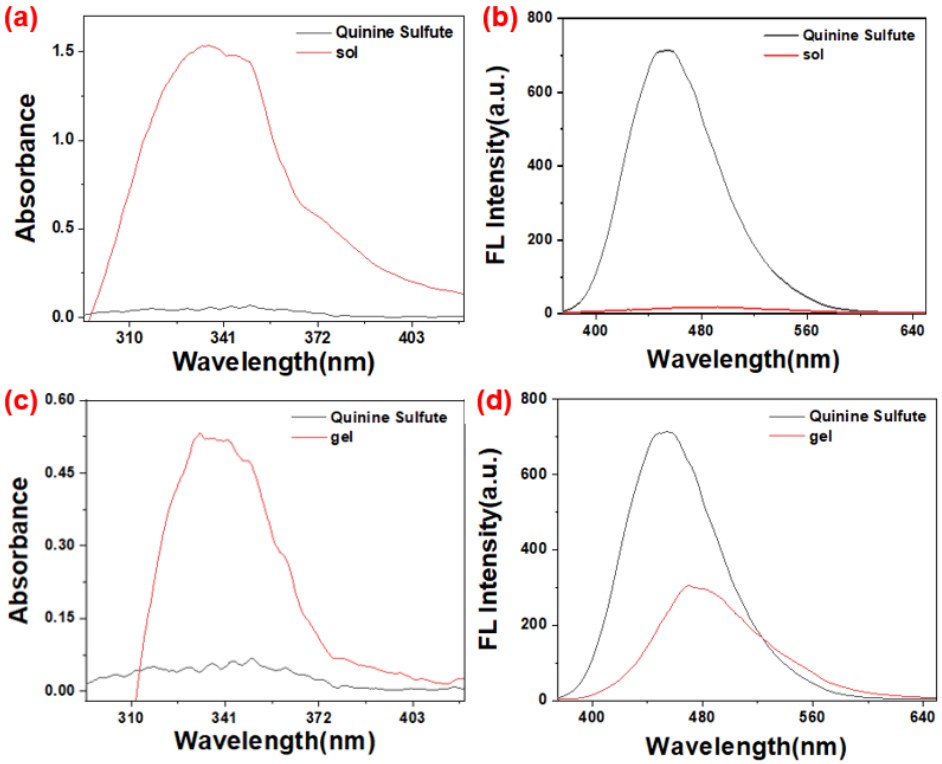

Fig. S12 Fluorescence quantum yield according to the corresponding formula (using quinoline sulfate as standard).

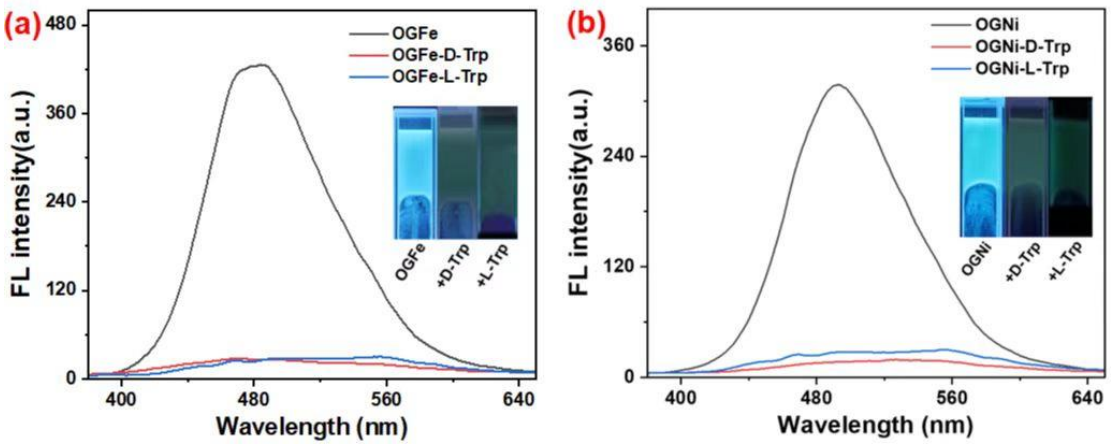

Fig. S13 The fluorescence spectra and photographs of (a) **OGFe** before and after addition of 1.0 equiv. L-Trp and D-Trp; (b) **OGNi** before and after adding of 1.0 equiv. L-Trp and D-Trp (cyclohexanol solution, 5%, w/v, λex = 365 nm).

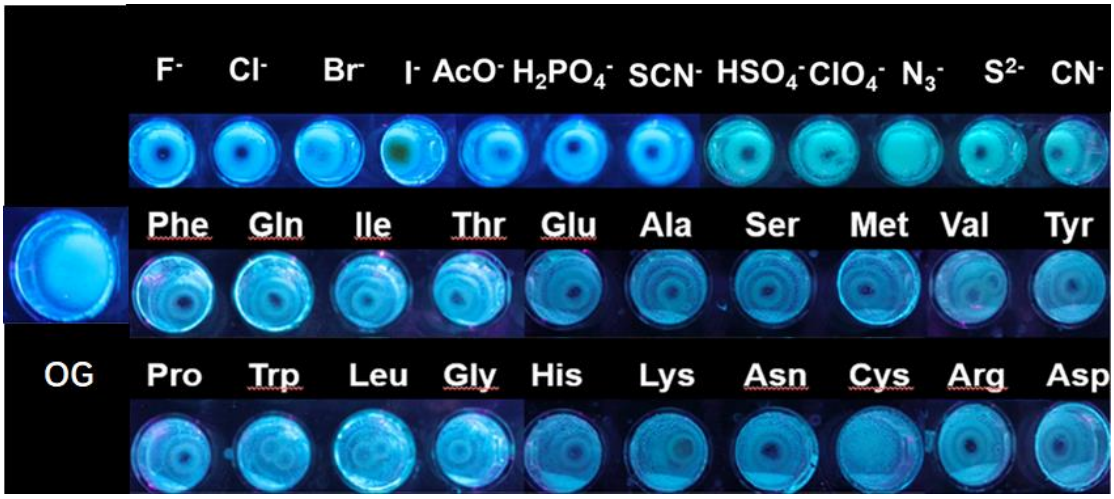

Fig. S14 Photographs of the fluorescence response of **OG** and **OG** in the presence of 1.0 equiv. different anions and amino acids respectively at room temperature under 365 nm UV light in cyclohexanol solution (5%, w/v).

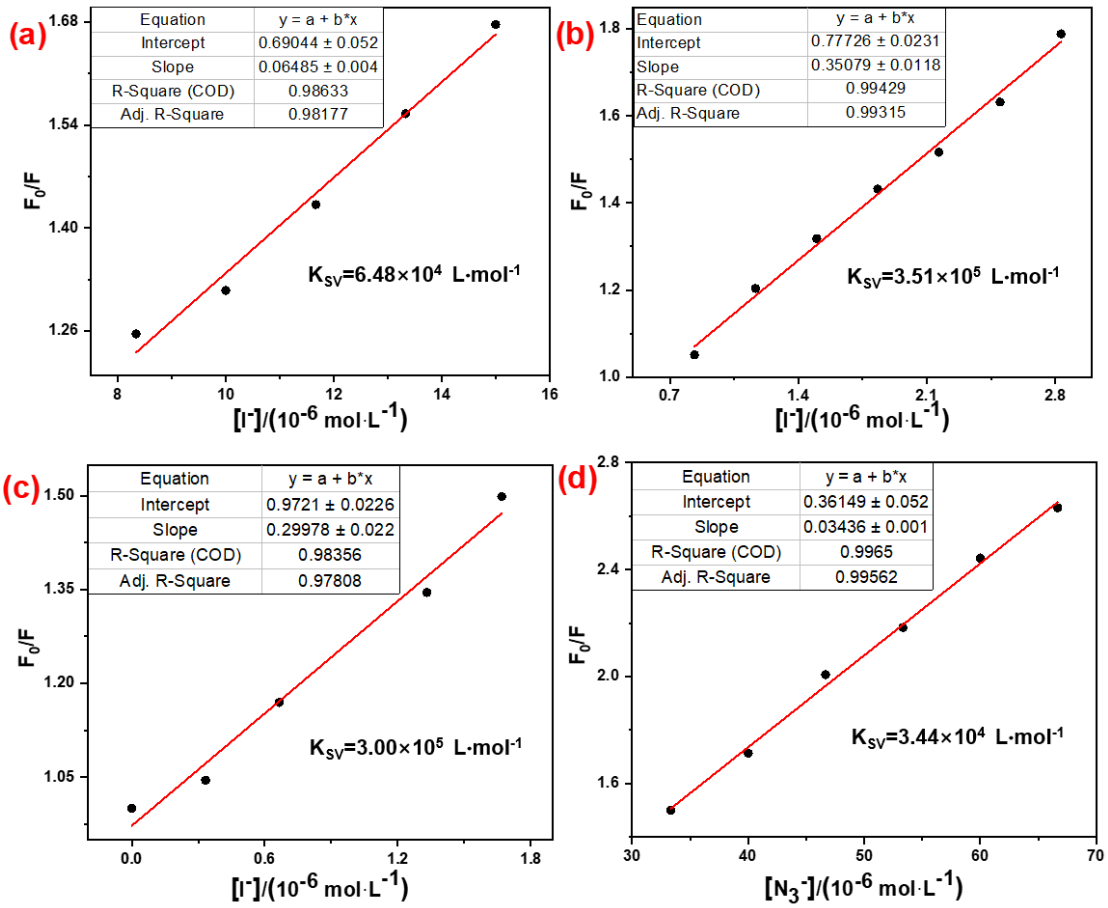

Fig. S15 Stern-Volmer plot of different metallogel with different anions. (a) **OGFe** with I⁻, (b) **OGCa** with I⁻, (c) **OGCu** with I⁻, (d) **OGCu** with N_3^- in cyclohexanol

solution (5%, w/v).

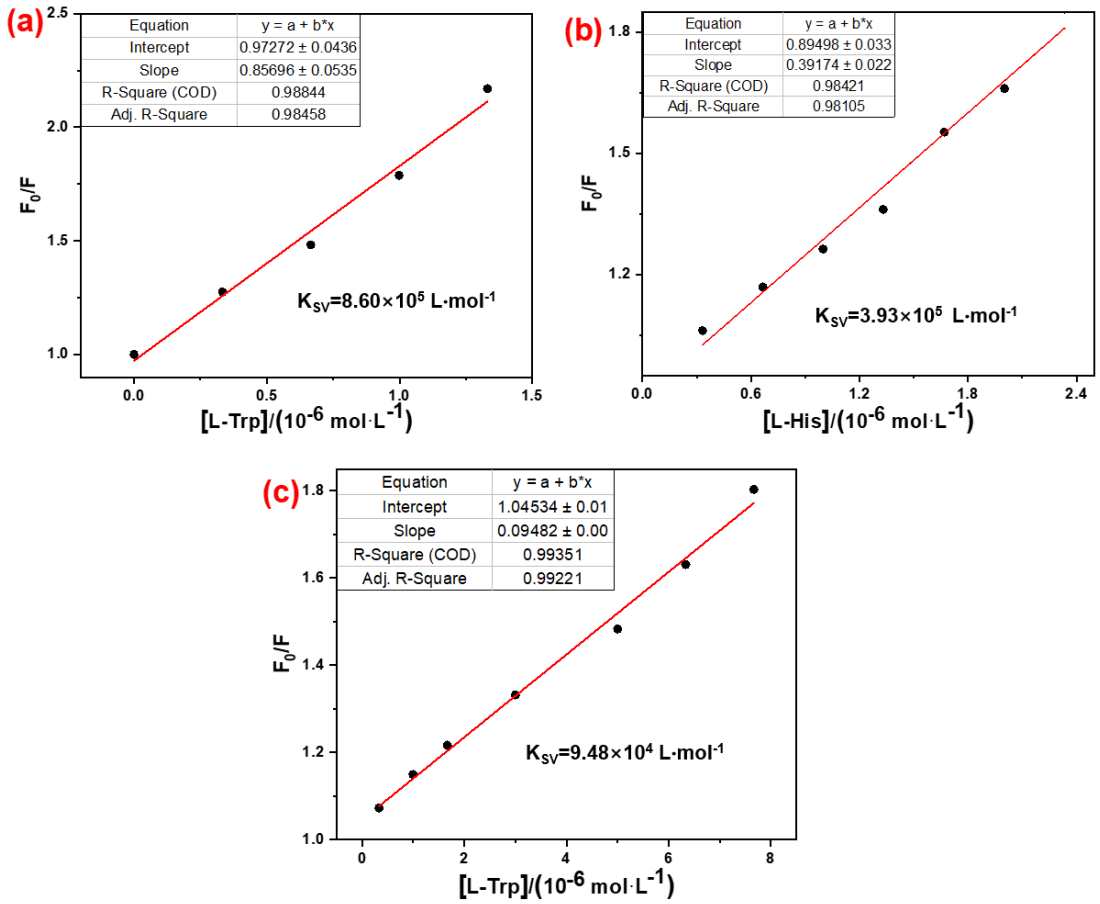

Fig. S16 Stern-Volmer plot of different metallogel with different amino acids. (a) **OGFe** with L-Trp, (b) **OGCo** withL-His, (c) **OGNi** with L-Trp in cyclohexanol solution (5%, w/v).

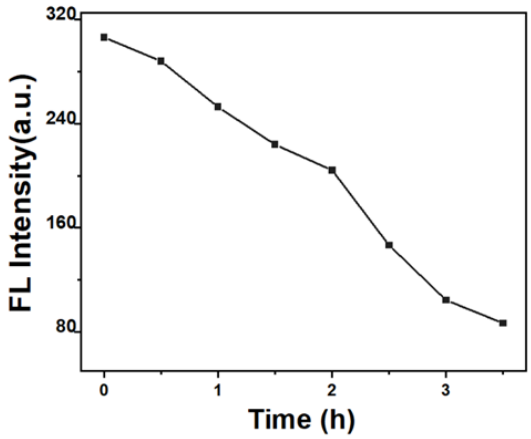

Fig. S17 Time-dependency cures of **OGCu-I** (cyclohexanol solution (5%, w/v)) with 0.076 equiv. I^- .

Table S1 Gelation behavior of gelator **G** in different solvents.

Entry	Solvent	State[a]	CGC[b](%)	T^{c}_{gel} (℃)
1	methanol	P	\	\
2	ethanol	P	\	\
4	n-butyl alcohol	G	6	47
5	n-propanol	S	\	\
6	n-hexanol	S	\	\
7	Formic acid	G	7	45
8	Acetic acid	S	\	\
9	Propanoic acid	S	\	\
10	Hexylic acid	P	\	\
11	Butyric acid	S	\	\
12	$CHCl_3$	s	\	\
13	DMF	S	\	\
14	Acetonitrile	P	\	\
15	DMSO	P		
16	Isopropyl alcohol	S	\	\
17	Cyclohexanol	G	**5**	**48-50**
18	Cyclohexane	P	\	\
19	n-hexane	P	\	\

a: G, P and S denote gelation, precipitation and solution, respectively.

b: the critical gelation concentration (5%, wt%, 10 mg/mL=1%).

c: the gelation temperature (℃)**.**

Table S2 Detection limits of the metallogel **OGMs** for target ions or amino acids.

Ions/amino acids	Refs	Solvent	LOD/nM
CN^-	43	DMSO	39.5
	44	DMSO/H_2O	77.1
	45	MeOH/H_2O	891.0
	46	MeOH/H_2O	150.0
	This work	Water solution	**10.6**
N_3^-	47	H_2O/THF	487.0
	48	DMSO	227.0
	49	HEPES buffer solution	100.0
	This work	Water solution	**46.6**
I^-	50	THF	7900.0
	51	Water solution	108.5
	52	Water solution	300.0
	53	Water solution	60.0
	This work	Water solution	**3.4/5.2**
L-Trp	54	MeOH/ HEPES buffer solution	243.0
	55	CH_3CN/H_2O	150.0
	56	DMSO/H_2O	283.0
	57	Phosphate buffer solution	5000.0
	This work	Water solution	**2.4/19.2**
L-His	58	HEPES buffer solution	100.0
	59	Acetate buffer solution	20.0
	60	PBS buffer solution	72.2
	61	Tris-HCL buffer solution	36.0
	This work	Water solution	**2.4**

Table S3 The fluorescence quantum yield of **OG** in cyclohexanol solution (5%, w/v) in different states

Compound	State	Absorbance	Integral Area	Refractive Index	QY
quinine sulfate	solution	0.036	62346.54	1.333	0.55
OG	sol	0.673	3574.787	1.478	0.000208
	gel	0.178	30053.29	1.478	0.065919